

# Impulse Excitation Study of Elasticity of Different Precipitated Microstructures in IN738LC at High Temperatures

A. Raman, Samuel Ibekwe, and Timothy Gabb

(Submitted June 20, 2003; in revised form January 18, 2005)

The elastic modulus of the cast superalloy IN738LC in various heat-treated conditions was determined with multiple specimens for each microstructure using the impulse excitation technique and the resonant frequencies while heating and cooling. Whereas the second and higher order harmonics were also excited in the high temperature range 700-1000 °C in 50 mm long specimens during controlled heating, analogous specimens 35 mm in length, impacted in similar fashion, did not excite the higher harmonics. Also, the 50 mm long specimens became excited and stayed in the second harmonic over broader temperature ranges during uncontrolled cooling inside the closed furnace. All precipitated conditions had nearly similar elastic data, varying from about 200 to 115 GPa, with small deviations, within 5%, found among multiple specimens of similar microstructures tested. Specimens with fine nano-size precipitates had a distinctly smaller rate of decrease in elastic modulus with increasing temperature, in contrast to a somewhat larger and nearly similar rate of decrease in specimens with coarse or medium-sized precipitates. This behavior is indicative of a larger average cohesive strength between the atoms and/or between the matrix and the precipitate particles in the former microstructure. The duplex size precipitate microstructure seemed to have both small and large drops in different specimens.

**Keywords** elastic softening, impulse excitation, resonant frequency, Superalloy IN738LC, Young's modulus at high temperatures

## 1. Introduction

Elastic modulus data for the cast nickel-based superalloy IN738LC was experimentally determined in an earlier study using the regular tensile test procedure (Ref 1). Those tests were performed at room temperature and at 650, 750, and 850 °C, using two specimens for each test for samples containing fine, medium, coarse, and duplex size (fine + medium)  $\gamma'$  precipitates. Tests were also performed at two different strain rates, one corresponding to low values and the other to somewhat higher values. Earlier results seemed to indicate that there was a slight, anomalous elastic hardening in the same temperature range (i.e., 450-850 °C), as for the secondary anomalous yield strength increase in IN738LC. Since the results seemed to be consistent and similar behavior had not been observed before, it was decided that experiments should be repeated and the elastic behavior of the alloy should be studied with various precipitate microstructures using an auxiliary technique. For this purpose, the impulse excitation technique for determining the elastic modulus was chosen. An analogous test procedure had been used by Bayerlein and Sockel (Ref 2) in their study

A. Raman, Materials Group, Mechanical Engineering Department, Louisiana State University, Baton Rouge, LA, 70803; Samuel Ibekwe, Mechanical Engineering Department, Southern University, Baton Rouge, LA, 70813; and Timothy Gabb, Glenn Research Center, NASA, Cleveland, OH, 44135. Contact e-mail: meraman@alpha2.eng.lsu.edu.

to determine the elastic constants of IN738LC in a similar temperature range for a single crystal of the alloy. This paper reports the results of the impulse excitation tests performed on suitably heat-treated IN738LC samples at the NASA-Glenn Research Center (Cleveland, OH).

## 2. Experimental

Small rectangular beam-type specimens of dimensions 3 × 4 × 50 mm were machined from cylindrical rod stock. These specimens were heat treated under vacuum in sealed silica tubes to give rise to the various precipitated microstructures. The heat treatment schedules are discussed in detail elsewhere (Ref 3). Briefly, the heat treatments consist of solution treating at 1200 °C for 4 h followed by a water quench (WQ), which results in a microstructure with fine nano-sized precipitates. Reheating at 900 and 1120 °C for 24 h enables precipitate growth and results in medium- and coarse-sized precipitates in the microstructure, respectively. The duplex precipitate distribution, having both fine nano-sized and medium-sized precipitates, results when the alloy with coarse-sized precipitates is heated for an additional 6 h at 1140 °C. The coarse precipitates dissolve partially into the matrix, giving the two different precipitate sizes. Heating the alloy at 1250 °C for 2 h and then water quenching results in the single phase supersaturated solid solution (SSSS) containing no detectable precipitates (Ref 3, 4).

The microstructures tested were of five different types with differences only in the size, shape, and distribution of the  $\gamma'$  precipitates. These five microstructures are identified as (a) specimen with supersaturated solid solution and no precipitates (SSSS); (b) fine specimens with ultra-fine, nano-sized precipitates (~70 nm); (c) medium specimens with medium-sized precipitates (~400 nm); (d) duplex specimens containing both

fine (~60 nm) and medium (~300 nm) sized precipitates; and (e) coarse specimens with fairly large-sized coarse precipitates (~700 nm). Precipitate size was determined by examining suitably polished and etched specimens in a scanning electron microscope (SEM).

Three specimens were tested for each condition, except for the SSSS where only one specimen was studied. Specimen surfaces were polished thoroughly, cleaned, and weighed. Their dimensions were also accurately measured. From the mass and size of each specimen, the mass density was automatically calculated by the data analysis program. Each specimen was tested separately, and a typical impulse excitation test lasted nearly 8 h. For the excitation analysis a GrindoSonic MK5 Industrial Instrument (J.W. Lemmens N.V., Leuven, Belgium) was used.

The impulse excitation technique uses a dynamic method to determine the elastic properties of a material (Ref 5). The experimental procedure consisted of hanging the specimen inside the equipment as a parallel beam and exciting it by means of an impact event at the middle of one of the larger surfaces using a tiny, pointed striker. The striker is propelled by an Ar jet stream when a gate valve holding it in place is opened. The specimen must be carefully located a couple of centimeters above the valve in a flat manner, approximately parallel to the bottom and top surfaces of the equipment chamber.

The specimen is hung as a free hanging beam from two fixed support rods, parallel to each other and approximately 50 cm apart, using fine Inconel wire. The rod assembly is moved in such a way as to bring the specimen to the proper position inside the chamber, aligning it exactly above the striker opening. Suitable guides enable such exact alignment. The specimen is thus positioned at the center of a vacuum furnace that can be evacuated in steps and filled with Ar if necessary. Tests can then be undertaken in vacuum or in a suitable gaseous environment. These experiments were performed in a vacuum. Throughout the experimental test program, the specimens can be viewed through a glass window in the front door of the chamber.

The unit has a programmable furnace controller. A computer program associated with the unit records all data and analyzes it upon the conclusion of each experimental run. The

data related to heating rate, ramp temperature, and holding time during the ramps can be fed into the computer at the outset, along with the data pertaining to the specimen identification, mass, and dimensions.

The maximum cut-off temperature can also be specified. Initially, impacts are made on the specimens by allowing the valve to open, thereby allowing the striker to hit the specimen. The acoustic waves are detected by a microphone, and after immediate analysis, the resonant frequency is displayed on the instrument monitor. Simultaneously, both the temperature and the corresponding resonant frequency are recorded. The specimen is then heated slowly at the programmed rate, and at different predetermined temperatures, the striker is activated and the resonance frequency data is collected and recorded.

The heating of the furnace is automatically stopped at the end of the heating cycle and once the maximum test temperature is reached. At this point, fresh Ar is flushed through the interior of the furnace three times. Thereafter, the furnace is allowed to cool naturally in vacuum. While cooling, the temperature inside the furnace is monitored and at selected temperatures the dynamic elastic modulus is measured. The data is manually recorded at this stage since the computer program has been turned off with the furnace after reaching the maximum test temperature. In this manner, data from excitation frequencies can be gathered at different temperatures while the specimen continuously cools. Note, however, that whereas the heating rate was controlled and the data obtained automatically at well-defined intervals, the data obtained during cooling are obtained without any control over the cooling rate. The cooling was obviously fast to start with at high temperatures but slowed progressively as the temperature dropped, taking considerably longer as it approached ambient conditions.

A computer data analysis program then displayed the data as temperature versus resonant frequency. The data were then used to calculate the dynamic elastic modulus of the specimen and a plot of  $E$  versus  $T$  was generated using the graphing software.

The dimensions of the specimen as well as its mass were used to compute the mass density. This information was used with Poisson's ratio of the material and the resonance frequency to compute the dynamic elastic modulus (Ref 5, 6).

**Table 1 Elastic modulus of various precipitate microstructures in IN738LC at selected temperatures**

Temperature °C	Elastic modulus, GPa													
	SSSS	Fine			Medium			Duplex(a)			Coarse			
25 (RT)	203.9	203.4	201.6	195.1(b)	203.7	216.1	199.5(b)	202.7	191.1	205.2	207.7(b)	211.1	208.6	198.7(b)
100	199.2	198.7	196.9	190.3(b)	(c)	211.4	195.2(b)	198.0	186.4	200.3	201.8(b)	206.4	204.0	194.5(b)
200	194.0	193.5	191.5	184.6(b)	193.9	205.8	189.3(b)	192.8	181.2	194.0	195.8(b)	201.1	198.7	188.7(b)
300	188.9	(c)	186.3	179.2(b)	188.9	200.5	184.1(b)	187.7	176.2	188.5	190.8(b)	195.9	193.6	183.3(b)
400	183.3	182.9	180.9	174.0(b)	183.5	194.9	179.0(b)	182.3	171.0	183.0	185.5(b)	190.4	188.1	178.0(b)
500	177.8	177.5	175.7	169.1(b)	178.2	189.2	173.4(b)	176.9	165.7	177.8	180.0(b)	184.6	182.5	172.8(b)
600	173.0	172.5	170.8	164.0(b)	171.9	182.7	166.9(b)	171.9	161.2	172.3	174.0(b)	178.1	176.1	166.2(b)
700	167.1	166.6	164.8	158.1(b)	164.9	175.6	160.3(b)	166.1	155.4	166.2	167.4(b)	(c)	169.1	159.4(b)
800	2nd(d)	(c)	157.8	150.9(b)	(c)	168.2	153.2(b)	2nd(d)	148.7	158.8	160.1(b)	(c)	2nd(d)	152.4(b)
900	2nd(d)	(c)	(c)	142.4(b)	2nd(d)	(c)	144.8(b)	(c)	(c)	(c)	151.7(b)	(c)	(c)	144.2(b)
1000	139.9	(c)	140.5	131.0(b)	137.8	148.8	133.1(b)	off(e)	128.8	142.0	139.4(b)	off(e)	off(e)	131.3(b)
1100(b)	off(e)	...	...	115.7(b)	...	...	116.3(b)	121.3	...	...	122.6(b)	...	...	115.5(b)

SSSS, supersaturated solid solution with no visible (in SEM at high magnification) precipitate content. Fine, specimen with very fine precipitates of size about 70 nm. Medium, specimen with medium size precipitates with size about 400 nm. Duplex, specimens with two distinct precipitate sizes, one fine of about 60 nm and the other, partially dissolved coarse precipitates of size about 300 nm. Coarse, specimens with coarse precipitates with size about 700 nm, (a) 3rd and 4th data values are for specimens with 50 and 35 mm length spans, respectively. (b) Data for specimens with length of about 35 mm. (c) Values lying between those of the first and second harmonics of vibration. (d) 2nd: value, not listed here, from the second harmonic data, calculated with the formula for the first harmonic; higher by a factor of about 7.6. (e) off: off-scale, shown as zero; computer program could not calculate the value

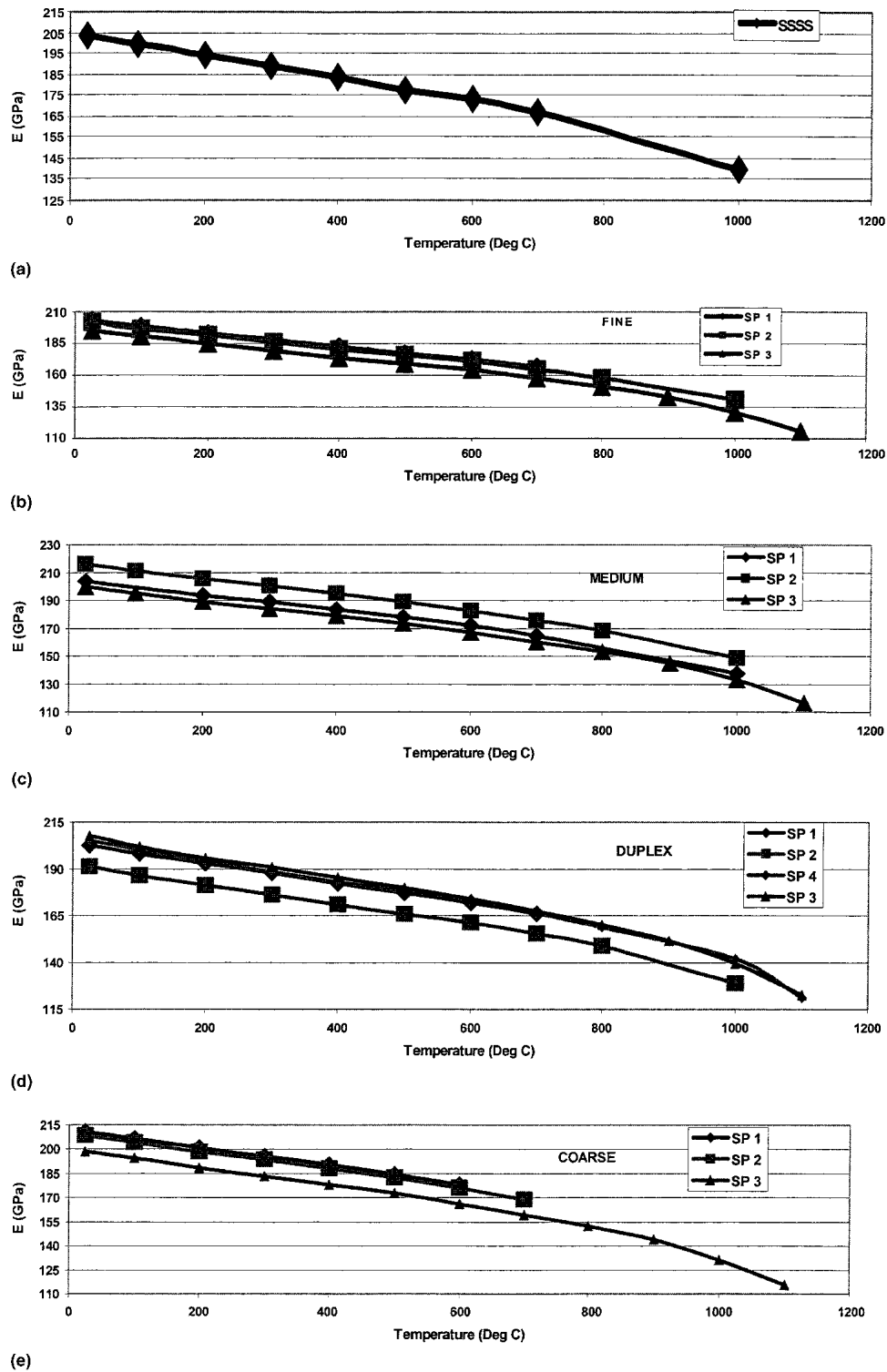


**Fig. 1**  $E$  versus temperature ( $T$ ) for the 50 mm long specimens with various precipitate microstructures: (a) SSSS, (b) fine, (c) medium, (d) duplex, and (e) coarse. The data from the first harmonic only is plotted.

$$E = a \left[ \frac{\rho L^4 f^2 S}{t^2 (1 + \alpha \Delta T)} \right] \quad (\text{Eq 1})$$

where  $a$  is conversion factor equal to 0.94642,  $\rho$  is the density ( $\text{kg/m}^3$ ),  $L$  is the specimen length (m),  $f$  is the resonant frequency (Hz),  $S$  is a shape factor which is dependent on Poisson's ratio,  $t$  is the specimen thickness (m),  $\alpha$  is the coefficient of thermal expansion of the specimen, and  $\Delta T$  is the tempera-

ture difference between room temperature and the test temperature.

### 3. Results and Discussion

Results obtained for the three sets of specimens of various microstructures are compiled in Table 1 for every  $100^\circ$  inter-

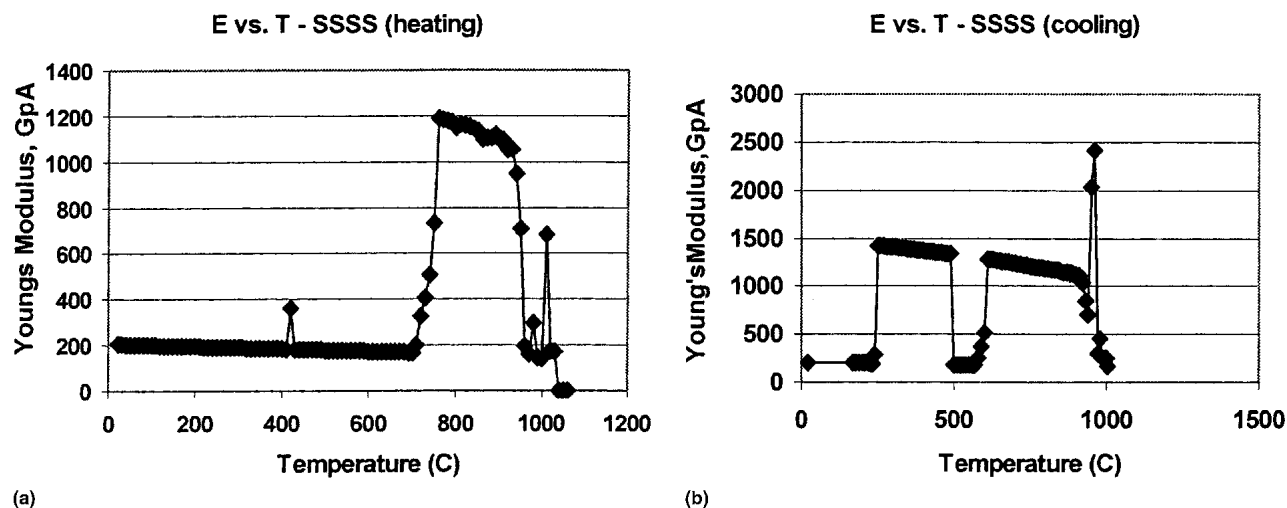


Fig. 2  $E$  versus  $T$  for the SSSS condition: (a) with controlled heating and (b) with natural (uncontrolled), continuous cooling

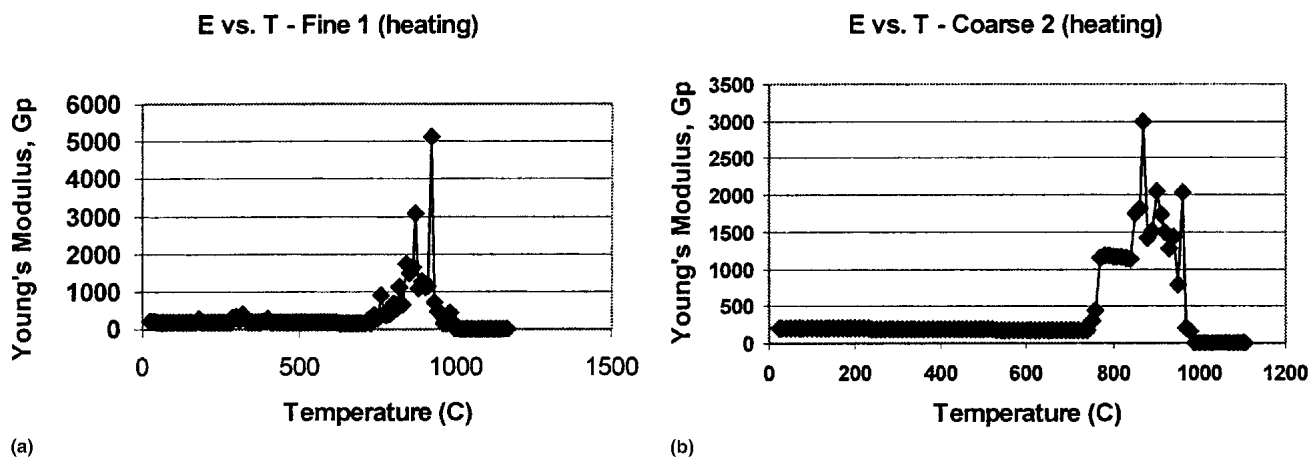


Fig. 3  $E$  versus  $T$  plots for heating showing shifting of excitation modes from the first harmonic: (a) fine #1 shows oscillatory movement of resonance frequency between first, second and third modes (in the range 710-990 °C); (b) coarse #2 shows shifting of mode to the third at 840 °C from the well-defined second mode (in the range 780-840 °C)

val. Whereas the first two sets of data for each condition correspond to specimens with a 50 mm beam length, the third set of data denoted with the footnote symbol (b) is for the specimen with a beam length of 35 mm. In the case of the duplex specimen, however, this corresponds to the fourth data set. The data given in Table 1 for specimens of various microstructures with 50 mm length are plotted in Fig. 1(a) to (e). The data from only the first harmonic are used in these plots.

Room temperature (RT) elastic modulus data for the various microstructures hovered around 200 GPa, although values as low as 191 GPa (duplex) and as high as 216 GPa (medium) were obtained on one of the specimens for each condition. Elastic constants given by Bayerlein and Sockel for IN738LC yielded 230 GPa for the elastic modulus at RT along the  $\langle 110 \rangle$  crystal directions (Ref 2). Data for the five heat-treatment conditions indicated that whereas the data from the first two sets were nearly consistent for the fine and coarse conditions, the data from the first two sets were noticeably different for medium and duplex samples.

In addition, for all samples in sets 1 and 2, specimens exhibited an overwhelming tendency to shift to the second mode of vibration when the temperature reached 700 °C during heat-

ing, e.g., Fig. 2(a) and 3(b). The samples became excited and stayed preferentially in the second mode over a broader temperature range while cooling from the high temperature. They stayed in the second mode till the temperature dropped to around 600 °C, at which time the excitation mode shifted back to the first. However, some of the specimens would switch again to the second mode at still lower temperatures, reverting back later to the first mode at around 200 °C. This characteristic behavior is illustrated for the SSSS condition in Fig. 2(b).

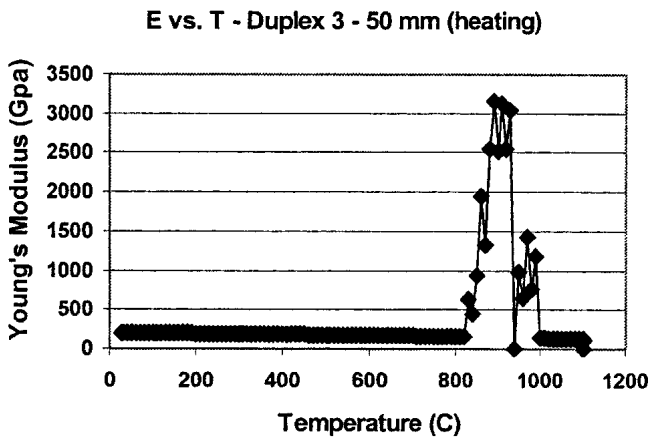
The extrapolated value of the modulus at RT from the higher harmonic is about 1540 GPa, which is about 7.55 times larger than the modulus value at RT obtained from the first harmonic. According to the beam excitation theory, the elastic modulus at RT should increase by a factor of 7.6 if the second harmonic of the beam is excited, by 29.2 if the third harmonic is excited, and by 79.8 if the fourth harmonic is excited (Ref 7). Thus, the result obtained from the higher harmonic proves it to be the second order harmonic. The RT elastic modulus obtained by using the amplification factor of 7.6 gives 202.6 GPa, which is close to the value obtained from the first harmonic.

It is also noteworthy that the transition from the first harmonic to the second harmonic does not occur abruptly at a

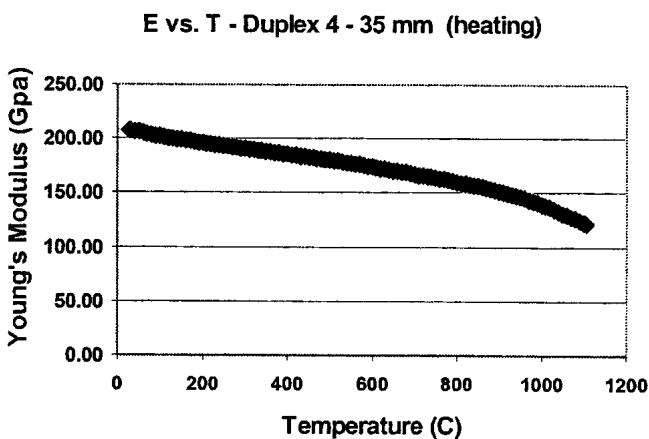
specific temperature; rather, it occurs smoothly (in some instances as shown in Fig. 2a) over a small temperature range, e.g., 700-760 °C. In actuality, both harmonics seem to become excited, and the net resonant frequency detected seems to be some value combining the two. However, in most instances an oscillatory shift in frequency and an excitation of higher harmonics (e.g., Fig. 3a) was encountered in the range 700-1000 °C during heating. It was also found infrequently to occur at much lower temperatures, around 300-400 °C, as in Fig. 2(a) and 3(a). The specimens seemed to prefer the second mode of excitation while cooling and stayed in this mode over a fairly broad temperature range, or split temperature ranges, in some instances, as already seen for the SSSS specimen. The reason for such a preference during cooling is not clear.

Also, the reasons for the transition from the first mode to the second one, and vice-versa, are not well understood. In a similar manner, mostly during heating, some of the specimens would exhibit a tendency to shift to the third mode, but mostly over a much narrower temperature range. Yet, a total shift to the third mode has not been detected in this study. Only the intermediate, mixed frequencies of excitation involving the third mode and the others have been obtained. Figures 3(a) and (b) illustrate this behavior.

Such shifts have not been encountered while testing ceramic specimens (35 mm beam length). Hence, an attempt was made



(a)

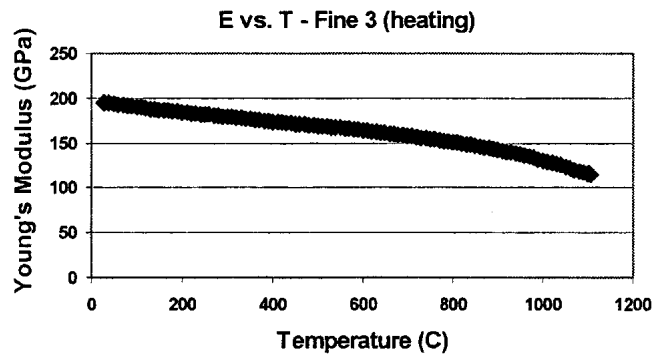


(b)

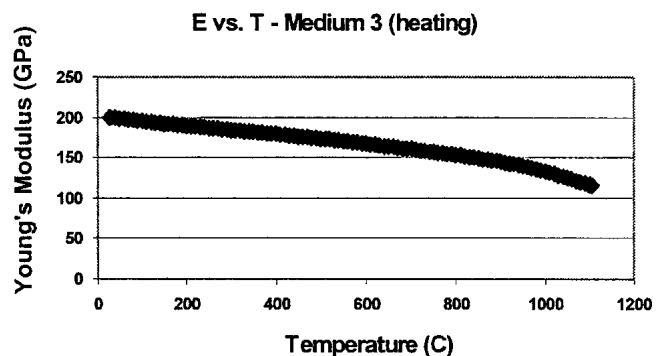
Fig. 4 *E* versus *T* plots for the duplex for heating: (a) specimen #3 of length 50 mm, (b) specimen #4 with length reduced to 35 mm; other parameters remain similar.

to perform the experiment on a duplex specimen first with a specimen of length 50 mm and then with a different specimen after reducing its length to 35 mm (i.e., removing 15 mm of span from a 50 mm long duplex specimen). Results are shown in Fig. 4(a) and (b). The specimen with the reduced length did not show any tendency to excite the second harmonic. The resultant *E* versus *T* curve is continuous throughout. Tests performed on the other three conditions of the alloy with the reduced length of 35 mm yielded similar plots of *E* versus *T* (Fig. 5a-c).

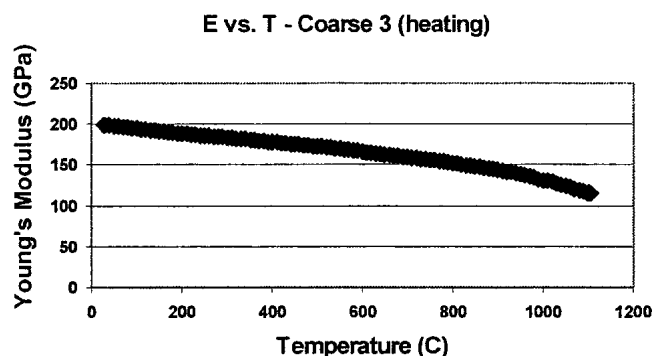
It is obvious from the plots of the reduced length specimens that the elastic modulus decreases uniformly over most of the temperature range until around 900 °C after which the decrease seems to accelerate. This can be attributed to the general softening of the matrix near the precipitate dissolution temperature range, or in more general terms, near the solidus temperature of the alloy. In all cases there is no increase in the elastic modulus near the anomalous hardening temperature of 750 °C.



(a)



(b)



(c)

Fig. 5 *E* versus *T* plots for the 35 mm long specimens with various microstructures: (a) fine, (b) medium, and (c) coarse

If the data from the three specimens for each condition are compared, it is found that two of the three data sets are very close to each other and their plots overlap (Fig. 1). One set of data is distinctly off. Thus, in the case of specimens with medium- and duplex-size precipitates, the data from the second specimen in each case are different by about 5%. The data are higher in the case of medium-sized precipitates, and lower in the case of duplex precipitates, compared with the mean value. This deviation, however, is negated by the data from the third specimen in each case, which gives values closer to those of the first specimen.

Another interesting result is that the elastic modulus values from the 35 mm long beam specimens are consistently smaller than those from the 50 mm long beam specimens for all cases other than for the duplex precipitate specimens (Table 1 and Fig. 1b-e). For the specimens in Fig. 1(d), the highest values of elastic modulus for the 35 mm span have been recorded. These values are somewhat consistent with the values of two of the 50 mm long beam specimens. Likewise, the values for the coarse-sized precipitate sample using the 35 mm beam specimen are distinctly lower than the values from the two 50 mm long beam specimens. In this case, the larger values obtained with the 50 mm beam span would make this condition anomalous, because from earlier data, based on thermal expansion test results (Ref 8), the specimen with the coarse precipitates had the lowest elastic modulus. This was probably due to the (001) preferred orientation. However, the results with the 35 mm beam span would, more or less, corroborate these earlier observations.

An analysis of the drops in elastic modulus values with analogous rising temperature up to 700 °C shows that both the SSSS and fine precipitate microstructures soften by the smallest amount, 36.8-37.0 GPa. However, the medium and coarse precipitate samples soften somewhat more, 39.0-39.5 GPa. Data from the duplex size microstructure seem to show both small (in the first and second sets) and large (in the third and fourth sets) elastic modulus drops. The largest drops, 40.5 and 40.3 GPa, occur for the second set of medium (50 mm beam specimen) and the fourth set of duplex (35 mm beam specimen) microstructures, respectively. Translating this behavior into thermal expansion would mean smaller increments in the thermal expansion coefficients for this temperature range for the SSSS and fine than for the medium and coarse precipitate microstructures that would have somewhat larger increments in their thermal expansion coefficients.

Results from the earlier thermal expansion studies (Ref 8) seem to be in line with this deduction for the SSSS microstructure. Since this microstructure would yield fine precipitates during heating, analogous results can be expected for the fine precipitate microstructure as well. Earlier results from the thermal expansion studies also indicated that the other microstructures, including the fine precipitate one, had somewhat larger increases in this temperature range. In addition, the duplex microstructure showed the smallest rise in the thermal expansion coefficient and was quite similar to the SSSS. Results

from the current study on the duplex microstructure specimens were varied. Specimens 1 and 2 with the 50 mm beam lengths showed a drop in elastic modulus of 36.6 and 35.7 GPa, while the third 50 mm long beam specimen and the 35 mm long beam specimen exhibited drops of 39.0 and 40.3 GPa, respectively, in the same temperature range. While the smaller drop of elastic modulus for this microstructure is compatible with the smallest rise in thermal expansion coefficient, the larger drop in elastic modulus for the 35 mm long specimen cannot be accounted for. It is even larger than the large drop obtained with the coarse precipitate microstructure described earlier.

From the results in this study, it can be concluded that the fine precipitate microstructure shows the least decrease in elastic modulus, whereas the coarse precipitate microstructure exhibits the maximum amount of elastic modulus decrease upon heating from ambient to 700 °C. The duplex-size precipitate microstructure behaves similarly to either the fine or the coarse microstructures in its elastic modulus softening behavior.

## Acknowledgments

Thanks are extended to NASA for providing financial support through the Grant No. NASA (00-01)-DGAP-08 and allowing access to NASA-GRC facilities to conduct experiments with the impulse excitation setup. Heartfelt thanks are also extended to Dr. Michael Nathal, GRC Division Head for enabling the collaboration, to John Miller of GRC for conducting the excitation experiments meticulously, and to Indranil Roy, Graduate Assistant at LSU, for help in heat-treating the samples and in the microstructural analysis.

## References

1. E. Balıkcı, "Microstructure Evolution and Its Influence on Thermal Expansion and Tensile Properties of the Superalloy IN738LC at High Temperatures," Ph.D. Dissertation, Louisiana State University, Baton Rouge, LA 1998
2. U. Bayerlein and H.G. Sockel, Determination of Single Crystal Elastic Constants from DS- and DR-Ni-Based Superalloys by a New Regression Method Between 20 °C and 1200 °C, *Superalloys 1992*, S.D. Antolovich, Ed., TMS, 1992, p 695-704
3. E. Balıkcı, A. Raman, and R.A. Mirshams, Influence of Various Heat Treatments on the Microstructure of Polycrystalline IN738LC, *Metall. Mater. Trans. A*, Vol 28 (No. 10), 1997, p 1993-2003
4. E. Balıkcı, R.A. Mirshams, and A. Raman, Microstructure Evolution in IN738LC in the Range 1120-1250 °C, *Z. Metallkd*, Vol 90 (No. 2), 1999, p 132-140
5. K. Heritage, C. Frisby, and A. Wolfenden, Impulse Excitation Technique for Dynamic Flexural Measurements at Moderate Temperature, *Rev. Sci. Instrum.*, Vol. 59 (No. 6), 1988, p 973-974
6. S. Spinner and W.E. Tefft, A Method for Determining Mechanical Resonance Frequencies and Calculating Elastic Moduli from These Frequencies, *Proc. ASTM*, Vol 61, 1961, p 1221-1238
7. Prof. Yitshak Ram, Mechanical Engineering, LSU, Baton Rouge, LA (private communication)
8. E. Balıkcı, A. Raman and R.A. Mirshams, Microstructure Effect on the Thermal Expansion of Polycrystalline Superalloy IN738LC, *Metall. Mater. Trans. A*, Vol 30 (No. 11), 1999, p 2803-2808